

conventional schemes such as those successfully used in solving the two-dimensional boundary-layer flows, thus avoiding the large computing time required for the exact solution. Additionally, the numerical solution is basically less restrictive in view of the nature of the approximations as compared with the existing methods.^{1,3} As this physical model is valid wherever the boundary-layer concept is applicable, present approximations should be effective for a wide class of vehicle geometries and flow conditions. With the governing equations written in central difference form and using the Crank-Nicholson type of implicit schemes, they have been programmed for numerical calculation.

For comparative purposes, the case presented in Ref. 3 was selected. It is seen that the heat-transfer rates as shown in Fig. 1 correspond very well considering the difference in the inviscid result used (Newtonian vs linear characteristic) and the streamline curvature computations (exact vs approximate). The shear stress in the streamwise and the crossflow directions similarly show good agreement as indicated in Fig. 2. However, the present calculation shows a definite maxima in the crossflow shear stress near $S/R = 4$. Available oil streak experimental results^{8,11} appear to favor the trend as predicted by the present calculation. Future computations using exact inviscid inputs^{9,10} will be needed to provide credence to this point of view.

In summary, an approximation based on a physical description of the boundary-layer flow has been devised. Its use has greatly simplified the task of numerical integration of the governing equations of three-dimensional, compressible laminar boundary layer. Numerical results have validated the effectiveness of the approximation and the computing time (to $S/R = 10$) per case (~ 2 min on CDC 6500) appears to be reasonable.

References

- ¹ Kang, S. W., Rae, W. J., and Dunn, M. G., "Effects of Mass Injection on Compressible, Three-Dimensional Laminar Boundary Layers," *AIAA Journal*, Vol. 5, No. 10, Oct. 1967, pp. 1738-1745.
- ² Trella, M. and Libby, P. A., "Similar Solutions for the Hypersonic Laminar Boundary Layer Near a Plane of Symmetry," *AIAA Journal*, Vol. 3, No. 1, Jan. 1965, pp. 75-83.
- ³ Fannelop, T. K., "A Method of Solving the Three-Dimensional Laminar Boundary Layer Equations with Application to a Lifting Reentry Body," *AIAA Journal*, Vol. 6, No. 6, June 1968, pp. 1075-1084.
- ⁴ Der, J., Jr. and Raetz, G. S., "Solution of General Three-Dimensional Laminar Boundary Layer Problem by an Exact Numerical Method," IAS Paper 62-70, Jan. 1962.
- ⁵ Stewartson, K., "Viscous Hypersonic Flow Past a Slender Cone," *The Physics of Fluids*, Vol. 7, No. 5, May 1964, pp. 667-675.
- ⁶ Vaglio-Laurin, R. and Miller, G., "On Three-Dimensional Laminar Boundary Layers with Large Cross-Flow," *AIAA Journal*, Vol. 8, No. 10, Oct. 1970, pp. 1822-1830.
- ⁷ Mayer, A., "Three-Dimensional Laminar Boundary Layers," *High Speed Aero/Dynamics and Jet Propulsion*, Vol. IV, Princeton University Press, Princeton, N.J., 1964, pp. 288-292.
- ⁸ Rainbird, W. J., Crabbe, R. S., and Jurewicz, "A Water Tunnel Investigation of the Flow Separation About Circular Cones at Incidence," LR-385, Sept. 1963, National Research Council of Canada, Ottawa, Canada.
- ⁹ Jones, D. J., "Numerical Solutions of the Flow Field for Conical Bodies in a Supersonic Stream," LR-507, July 1968, National Research Council of Canada, Ottawa, Canada.
- ¹⁰ Rakich, V. V. and Cleary, J. W., "Theoretical and Experimental Study of Supersonic Steady Flow Around Inclined Bodies of Revolution," *AIAA Journal*, Vol. 8, No. 3, March 1970, pp. 511-518.
- ¹¹ Stetson, K. F. and Friberg, E. G., "Surface Conditions in the Leeward Region of a Blunt Cone at Angle of Attack in Hypersonic Flow," ARL-69-0114, July 1969, ARL, Dayton, Ohio.

Shock Standoff Distances and Mach-Disk Diameters in Underexpanded Sonic Jets

W. DAVIDOR* AND S. S. PENNER†

University of California, San Diego, La Jolla, Calif.

Nomenclature

d_e = nozzle-exit diameter
 d_s = Mach-disk diameter
 p = pressure
 x = distance downstream of the nozzle-exit location
 γ = isobaric to isochoric heat-capacity ratio
 ξ = x/d_e

Subscripts

1 = upstream chamber conditions
 a = downstream (ambient) conditions

Introduction

A NUMBER of theoretical¹⁻⁴ and experimental^{1,5-7} studies has been published on the relation between pressure ratio and shock standoff distance. In particular, extensive compilations of experimental measurements have been published by Lewis and Carlson⁶ and by Crist, Sherman, and Glass,⁷ who noted that the ratio of stagnation pressure (p_1) to ambient pressure (p_a) was proportional to the square of the dimensionless ratio (ξ) of downstream distance (x) divided by the exit diameter (d_e) of a sonic nozzle; the proportionality constant was found⁷ to be equal to 2.4 and was independent of the ratio of isobaric to isochoric specific heat (γ).

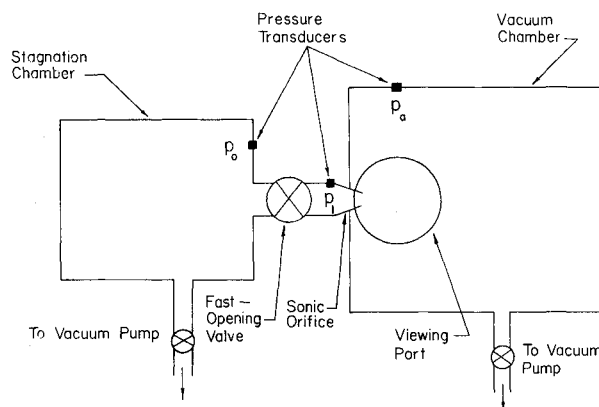


Fig. 1 Schematic diagram of the blow-down tunnel used for determining shock standoff distance as a function of pressure ratio. Volume of stagnation chamber = 524 cm³; volume of vacuum chamber = 7054 cm³; exit diameter of sonic nozzle = 0.680 cm; entrance diameter of sonic nozzle = 2.86 cm; the fast-opening valve is a shock-actuated valve which opens completely in 20 to 25 msec; pressure-transducer readings were accurate to about $\pm 5\%$. The initial pressure p_1 was between 11.75 and 13.25 psia with $p_a \approx 0.8$ psia.

Received December 17, 1970; revision received April 12, 1971. These studies have been supported under Project Themis and were sponsored by the Air Force Office of Scientific Research, Office of Aerospace Research, U.S. Air Force, under Contract F44620-68-C-0010. The authors are indebted to K. G. P. Sulzmann for assistance with the experimental studies and for helpful discussions.

* Assistant Research Engineer, Department of the Aerospace and Mechanical Engineering Sciences.

† Professor of Engineering Physics, Department of the Aerospace and Mechanical Engineering Sciences. Fellow AIAA.

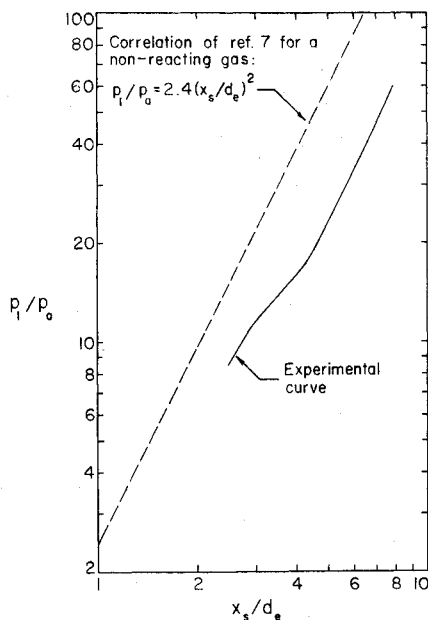


Fig. 2 Representative experimental results for p_1/p_0 as a function of x_s/d_e for mixtures of NO_2 and N_2O_4 .

Crist, Sherman, and Glass⁷ have also presented an empirical correlation between pressure ratios p_1/p_0 and the ratios of Mach-disk diameters d_s to nozzle-exit diameters d_e for nonreacting gases. Their correlation curves are notably dependent on γ with d_s/d_e increasing substantially as γ is decreased.

Shock Standoff Distance

We have performed experimental measurements of shock standoff distances and Mach-disk diameters in a blow-down tunnel with mixtures of NO_2 and N_2O_4 as working fluid. The apparatus is described in the legend to Fig. 1. With an experimental time resolution of 10^{-2} sec, the flow processes may be considered to be pseudo-steady in an experiment with a duration of about 1.5 sec. The chemical relaxation times for equilibration between NO_2 and N_2O_4 are of the order of microseconds for our experiments.⁸ The utility of the pro-

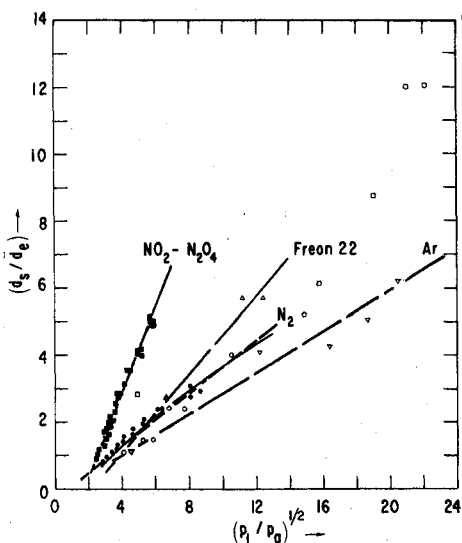


Fig. 3 Data showing the reduced Mach-disk diameters (d_s/d_e) as functions of $(p_1/p_0)^{1/2}$. The following symbols are used: curve for N_2 , from Love, et al.⁵; Δ Freon 22, from Crist, et al.⁷; \square CO_2 , from Crist et al.⁷; \circ N_2 , from Crist et al.⁷; \bullet N_2 , present study; ∇ Ar, from Crist et al.⁷; \blacksquare $\text{NO}_2\text{-N}_2\text{O}_4$, present study.

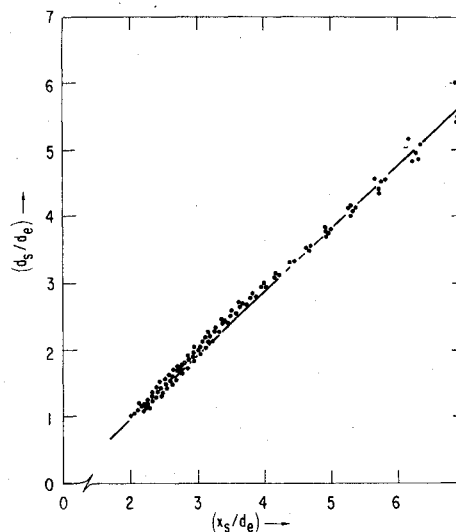


Fig. 4 Reduced Mach-disk diameters (d_s/d_e) as functions of reduced downstream distance (x_s/d_e) for mixtures of NO_2 and N_2O_4 ; initial values of $p_1 \approx 11.75$ to 13.25 psia, initial value of $p_0 \approx 0.8$ psia.

cedure was verified for nitrogen-flows. Standoff distances were determined photographically by using a movie camera. Representative experimental results are plotted in Fig. 2 for $\text{NO}_2\text{-N}_2\text{O}_4$ mixtures. The measurements on this reactive-gas system were reproducible within $\pm 10\%$ for p_1/p_0 at fixed measured distances of x_s/d_e .

The observed difference between the shock standoff distance vs pressure correlation for the $\text{NO}_2\text{-N}_2\text{O}_4$ system and for nonreacting gases is associated with large temperature changes occurring⁹ in the rapidly-reacting system which we have studied.

Mach-Disk Diameters

The previously published data on Mach-disk diameters have been replotted in Fig. 3, together with new experimental results for N_2 and for the reacting system $2\text{NO}_2 \rightleftharpoons \text{N}_2\text{O}_4$. Interpolation between the data plotted in Fig. 3 shows that our reacting system behaves like a gas mixture with an effective value of $\gamma = 1.12 \pm 0.02$.

Data of d_s/d_e as functions of x_s/d_e are shown in Fig. 4 for the $\text{NO}_2\text{-N}_2\text{O}_4$ system. Reference to Fig. 4 indicates that the experimental results are in accord with the idea that the observed Mach-disk diameters fall accurately within an expanding cone.

Our experimental findings on Mach-disk diameters may be accounted for on the basis of heuristic arguments that are similar to those appearing in previous publications.⁷

References

- Adamson, T. C., Jr. and Nicholls, J. A., "On the Structure of Jets from Highly Underexpanded Nozzles into Still Air," *Journal of Aerospace Sciences*, Vol. 26, 1959, pp. 16-24.
- Eastman, D. W. and Radtke, C. P., "Location of the Normal Shock Wave in the Exhaust Plume of a Jet," *AIAA Journal*, Vol. 1, No. 4, April 1963, pp. 918-919.
- Bowyer, J., D'Attore, L., and Yoshihara, H., Space Science Lab. Report GDA 63-0586, 1963, General Dynamics/Astronautics, San Diego, Calif.
- Abdelhamid, A. N. and D. S., Dosanjh, "Mach Disk and Riemann Wave in Underexpanded Jet Flow," *AIAA Paper* 69-665, San Francisco, Calif., 1969.
- Love, E. S., Grigsby, C. E., Lee, L. P., and Woodling, M. J., "Experimental and Theoretical Studies of Axisymmetric Free Jets," TR-R6, 1959, NASA.
- Lewis, C. H., Jr. and Carlson, D. J., "Normal Shock Location in Underexpanded Gas and Gas-Particle Jets," *AIAA Journal*, Vol. 2, No. 4, April 1964, pp. 776-777.

⁷ Crist, S., Sherman, P. M., and Glass, D. R., "Study of Highly Underexpanded Sonic Jet," *AIAA Journal*, Vol. 4, No. 1, Jan. 1966, pp. 68-71.

⁸ Wegener, P. P., "Supersonic Nozzle Flow with a Reacting Gas Mixture," *The Physics of Fluids*, Vol. 2, 1959, pp. 264-275.

⁹ Penner, S. S., Davidor, W., and Sulzmann, K. G. P., "Expansion of Nonreacting and Reacting Ideal Gases Between Interconnected Chambers," *American Journal of Physics*, Vol. 39, 1971, to be published.

Effect of Ring Out-of-Plane Bending Stiffness on Thermal Buckling Prediction for Ring-Stiffened Cylinders

DAVID BUSHNELL*

Lockheed Palo Alto Research Laboratory, Palo Alto, Calif.

A NUMBER of papers have been written on the thermal buckling of ring-stiffened cylinders in which the rings are treated as discrete.¹⁻⁴ The analyses were motivated by problems encountered in space shuttle and supersonic and hypersonic aircraft design. These vehicles are subjected to thermal transients such that the thin skin heats up while the more massive rings remain cold. Radial expansion of the skin is thus prevented in the neighborhood of the rings, giving rise to rapidly varying hoop compressive stresses there. It has been shown both theoretically¹⁻⁴ and experimentally² that buckling of the hot skin can occur in these narrow boundary-layer regions adjacent to the cool rings. Because of the narrowness of the region under hoop compression, buckling occurs with many waves around the circumference.

Analyses of this problem to date have included rings as discrete and eccentric (ring centroid not on shell reference surface). The rings have been modeled as "line" structures with certain extensional and bending properties for deformations in the plane of the rings. (Z, θ directions in Fig. 1.) The effect on buckling loads of ring out-of-plane bending stiffness (see Fig. 1) has generally been neglected.

The purpose of this Note is to demonstrate the importance of including out-of-plane bending stiffness of the ring in thermal buckling analyses. Comparisons are made for three configurations analyzed by Chang and Card.³ These configurations are shown in Figs. 2 and 3. Figures 4-6 show theoretical results obtained from the BOSOR3 computer program⁵ in which the "out-of-plane" moments I_z and I_{zz}

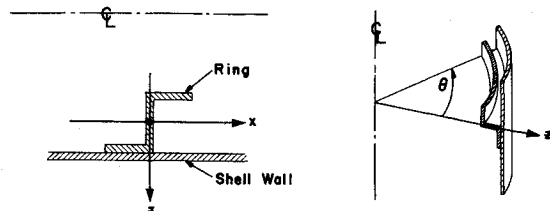


Fig. 1 Section of cylinder with internal ring. Out-of-plane bending refers to motion in x direction which varies harmonically around the circumference but involves no warping of the ring cross section.

Received March 19, 1971. Research sponsored by Lockheed Independent Research Program. I wish to express my appreciation to M. Card, who ran some cases and shared his thoughts with me on the physics of these thermal buckling problems.

* Staff Scientist. Member AIAA.

Shell & Ring Moduli: $E = 26.5 \times 10^6$ psi
Poisson's Ratio: $\nu = 0.3$
Thermal Expansion Coefficient: $\alpha = 7.95 \times 10^{-6}/^\circ\text{F}$
Case 1: $\ell = 3.075$ in Case 2: $\ell = 1.025$ in

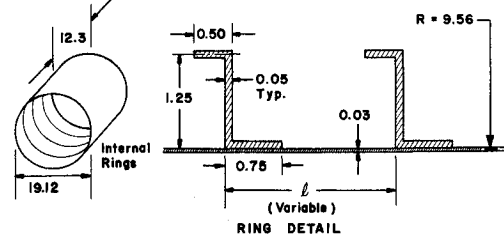


Fig. 2 Geometry of ring-stiffened cylinders, cases 1 and 2. Dimensions are in inches.

Shell Modulus: $E = 14.5 \times 10^6$ psi Ring Modulus: $E = 16.4 \times 10^6$ psi
Poisson's Ratio: $\nu = 0.32$
Thermal Expansion Coefficient: $\alpha = 5 \times 10^{-6}/^\circ\text{F}$

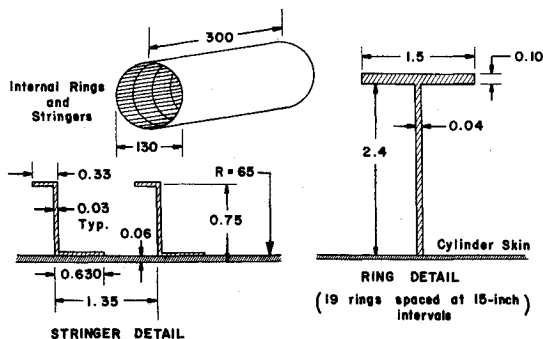


Fig. 3 Geometry of ring- and stringer-stiffened cylinder, case 3. Dimensions in inches.

are included in one case and neglected in the other. Torsional stiffness and ring cross section warping are neglected in all cases. Half of the shells are analyzed, with symmetry conditions in the prebuckling analysis and antisymmetry conditions in the buckling analysis being imposed at the symmetry plane.

Ninety-seven finite-difference mesh points are used in the analysis corresponding to Figs. 2 and 4. The shell in Fig. 3 is analyzed as consisting of two segments with 97 points in the first segment and 91 points in the second.

The most important effect is from the ring out-of-plane moment of inertia I_z . As seen from Eqs. (15), (17c), and

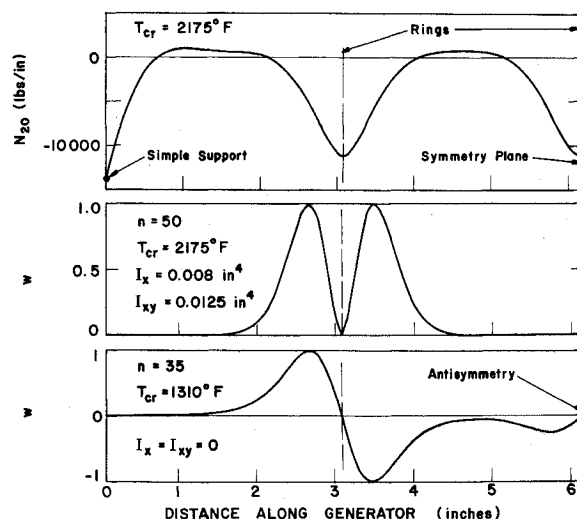


Fig. 4 Prebuckling hoop stress resultant N_{20} , buckling temperatures T_{cr} , circumferential waves n , and modes for case 1 (ring spacing = 3.075 in., see Fig. 2).